Metallic spin glasses

1996 J. Phys.: Condens. Matter 8 9723

(http://iopscience.iop.org/0953-8984/8/48/005)

J. Phys.: Condens. Matter **8** (1996) 9723–9741. Printed in the UK

Metallic spin glasses

Subir Sachdev and N Read

Department of Physics, Yale University, PO Box 208120, New Haven, CT 06520-8120, USA

Received 3 September 1996

Abstract. Recent work on the zero-temperature phases and phase transitions of strongly random electronic systems is reviewed. The transition between the spin glass and quantum paramagnet is examined, for both metallic and insulating systems. Insight gained from the solution of infinite-range models leads to a quantum field theory for the transition between a metallic quantum paramagnetic and a metallic spin glass. The finite-temperature phase diagram is described and crossover functions are computed in mean-field theory. A study of fluctuations about mean field leads to the formulation of scaling hypotheses.

1. Introduction

The vast majority of the existing theoretical and experimental work on spin glasses [1] has been in regimes where quantum effects can be almost entirely neglected, and both the statics and dynamics can be described by classical statistical mechanics models. This earlier work has focused on the paramagnetic phase not too far above the spin-glass transition temperature, T_c, and on the phase with spin-glass order with temperatures $T < T_c$. Thermal fluctuations then dominate, and the typical relaxation frequency, ω, satisfies $\hbar\omega \ll k_B T$, justifying the use of classical models. One important consequence of this classical behaviour is that the coupling between spin and charge fluctuations is rather weak; whether the frozen spins in the spin-glass phase are in a metallic, or an insulating, host is not of direct importance in theories of the formation of the spin-glass phase, or of its critical fluctuations. The metallic systems do have a longer-range RKKY interaction between the spins, but this does not fundamentally differentiate between the basic theoretical frameworks used to describe the two cases.

The situation is quite different when we vary T_c as a function of some tuning parameter (e.g. pressure, doping concentration of spins, or disorder) r, and examine the regime where $T_c(r)$ becomes much smaller than a typical microscopic exchange constant [2]. In particular, it may be possible to reach an $r = r_c$ at which we first have $T_c(r_c) = 0$; we will choose an overall shift in the value of r so that $r_c = 0$. For $r > 0$, then, the system is a paramagnet at all temperatures, including at $T = 0$. Considering the situation precisely at $T = 0$, the ground state undergoes a phase transition, from a spin glass ($r < 0$) to a paramagnet ($r > 0$), which is driven entirely by quantum fluctuations and disorder. Under these circumstances, as is described in more detail below, quantum effects play a fundamental role over a substantial portion of the T, r plane (and not just at $T = 0$). Concomitantly, the coupling between spin and charge fluctuations becomes much more important. It is now essential to specify whether the spin-glass and paramagnetic phases are metallic or insulating, as the effective theory of spin fluctuations is quite different in the two cases.

0953-8984/96/489723+19$19.50

In this paper, we will review recent work on insulating and metallic quantum spin glasses, highlighting the physical origin of the differences between the two cases. The emphasis will be on the metallic case, primarily because it is of greater experimental interest in the context of rare-earth intermetallic compounds described elsewhere in this Special Issue. A few results described here have not been explicitly obtained before, but they are straightforward consequences of work published earlier.

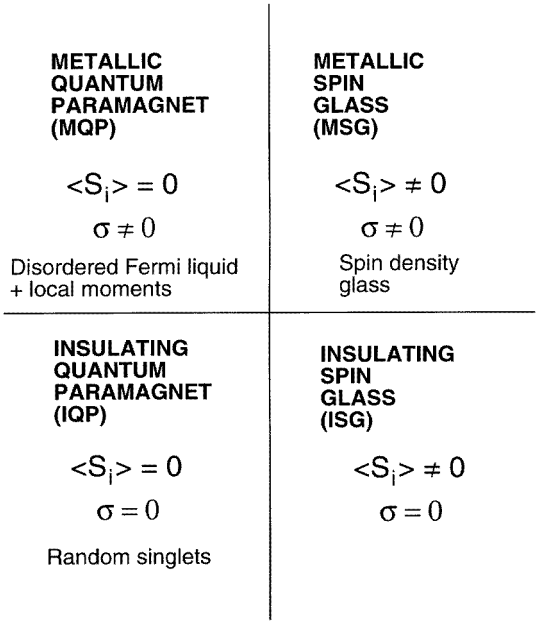

Figure 1. A schematic diagram of the $T = 0$ phases of a strongly random electronic system in three dimensions described e.g. by the Hamiltonian (1). The average moment, $\langle S_i \rangle$, when non-zero, varies randomly from site to site. The conductivity is denoted by σ.

2. General considerations

It is useful to begin by making a few general remarks on the expected phases, and their properties, of *strongly* random electronic systems in three dimensions. For concreteness, consider the $T = 0$ properties of the following Hamiltonian:

$$H = -\sum_{i<j,\alpha} t_{ij} c^{\dagger}_{i\alpha} c_{i\alpha} - \sum_{i<j,\mu} J^{\mu}_{ij} S_{i\mu} S_{j\mu} + H_{int} \tag{1}$$

where $c_{i\alpha}$ annihilates an electron on site i with spin $\alpha = \uparrow, \downarrow$, and the spin operator $S_{i\mu} \equiv \sum_{\alpha\beta} c^{\dagger}_{i\alpha} \sigma^{\mu}_{\alpha\beta} c_{i\beta}/2$ with σ^{μ} the Pauli matrices. The sites are placed in three-dimensional space and labelled by i, j, the hopping matrix elements t_{ij} are short ranged and possibly random, and the J^{μ}_{ij} are random exchange interactions, possibly with spin anisotropies. The remainder H_{int} includes other possible short-range interactions between the electrons: we will not need to specify them explicitly.

Figure 1 shows a possible $T = 0$ phase diagram of H as its couplings are varied. We have only identified phases between which it is possible to make a sharp distinction. The phases are determined by the behaviour of their spin and charge fluctuations. Charge

transport is characterized by the $T = 0$ value of the conductivity, σ; if $\sigma = 0$ the phase is an insulator, and it is metallic otherwise. For the spin sector, the uniform spin susceptibility is not a useful diagnostic (as will become clear below), and we distinguish phases by whether the ground state has infinite memory of the spin orientation on a site or not. The time-averaged moment on a given site is denoted by $\langle S_i \rangle$ (we will generally drop vector indices, μ, ν except where needed) and it can either vanish at every site, or take a non-zero value which varies randomly from site to site. The average over all sites will be denoted by $\overline{\langle S_i \rangle}$, and will be non-zero only in ferromagnetic phases, which we will not consider here.

The four phases in figure 1 are as follows.

(1) THE METALLIC QUANTUM PARAMAGNET (MQP). More simply known as the familiar 'metal', this phase has

$$\sigma \neq 0 \qquad \langle S_i \rangle = 0. \tag{2}$$

The charge transport occurs through quasiparticle excitations (which also carry spin) which can be described by a disordered version of Fermi-liquid theory [3]: the quasiparticles still obey a transport equation as in Landau's theory but have wave functions which are spatially disordered. However, it is also necessary to include a finite concentration of local spin moments to obtain a complete description of the low-energy spin excitations [4]. These local moments are created by relatively weak fluctuations in the disorder, and interact with each other and the conduction electrons via spin exchange. Although the spin fluctuations on the local moment sites are relatively slow, they eventually lose memory of their orientation, and we always have $\langle S_i \rangle = 0$.

(2) THE INSULATING QUANTUM PARAMAGNET (IQP). This phase has

$$\sigma = 0 \qquad \langle S_i \rangle = 0 \tag{3}$$

and is accessed by a metal–insulator transition from the MQP phase. It is also referred to as the 'random singlet' phase [5], the name describing spin-singlet bonds between pairs of spins. Breaking any of these singlet bonds costs an energy which has a broad distribution, with significant weight at low energy. The large density of low-energy spin excitations means that the spin susceptibility is quite large, and may even diverge as $T \to 0$ (this can also happen in the MQP phase, as argued by Bhatt and Fisher (see [4])). This is the reason we have not used the spin susceptibility as a diagnostic for the phases.

(3) THE METALLIC SPIN GLASS (MSG). This phase has

$$\sigma \neq 0 \qquad \langle S_i \rangle \neq 0 \tag{4}$$

and is accessed from the MQP by a spin-freezing transition. The local moments of the MQP phase now acquire a definite orientation, and retain memory of this orientation for infinite time. The Fermi-liquid quasiparticle excitations are still present and are responsible for the non-zero σ; the frozen moments appear as random local magnetic fields to the itinerant quasiparticles. Alternatively, we may view the spin-freezing transition as the onset, from the MQP phase, of a spin-density wave with random offsets in its phase and orientation, as appears to be the case in recent experiments [6]; this suggests the name '*spin-density glass*'. Although there are quantitative differences between these two points of view, there is no sharp or qualitative distinction and the two pictures are expected to be continuously connected. The latter point of view was explored by Hertz [7] some time ago, but he did not focus on the vicinity of the $T = 0$ transition between the MSG and MQP phases. An infinite-range model with a MSG phase was studied in reference [8] with a static *ansatz* for the order parameter. Here we will review the recent complete solution for the MSG phase

and the MSG–MQP transition in the infinite-range model [9, 10], the Landau theory for the short-range case [11, 9], and the consequences of fluctuations about the mean-field theory.

(4) THE INSULATING SPIN GLASS (ISG). This phase has

$$\sigma = 0 \qquad \langle S_i \rangle \neq 0. \tag{5}$$

Charge fluctuations are unimportant, and the collective frozen spin configuration is expected to be well described by an effective classical spin model. Examples of phases of this type may be found in reference [1].

Let us emphasize that the above discussion was restricted to $T = 0$, and thus describes only the ground-state properties of H. Indeed, all of the ground states have been studied earlier, and we shall have little to add to their description here. Our focus will primarily be on the finite-T properties in the vicinity of quantum phase transitions between the phases. As we will see, this finite-T behaviour can be quite non-trivial and remarkably rich; our results are summarized in figure 2 and will be discussed in more detail later. The possibility that such finite-T crossovers may offer an explanation of the unusual properties of lightly doped cuprates (and perhaps other strongly correlated systems) was discussed in reference [12].

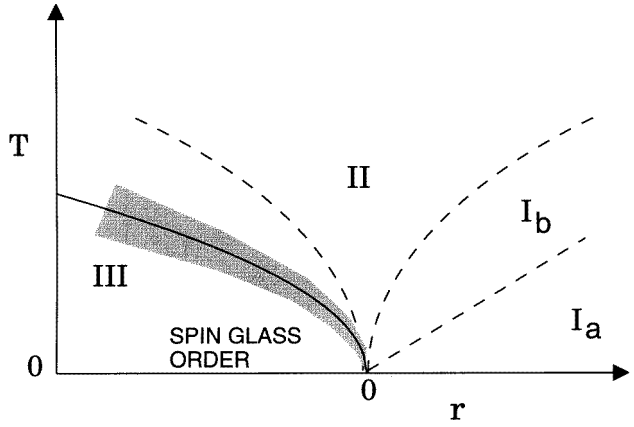

Figure 2. The phase diagram of a metallic spin glass as a function of the ground-state tuning parameter r and temperature T. In the notation of figure 1, the $T = 0$ state is a MSG for $r < 0$ and a MQP for $r > 0$. The full line is the only thermodynamic phase transition, and is at $r = r_c(T)$ or $T = T_c(r)$. The quantum critical point is at $r = 0$, $T = 0$, and is described by a continuum quantum field theory (CQFT). The dashed lines denote crossovers between different finite-T regions of the CQFT: the low-T regions are Ia, Ib (on the paramagnetic side) and III (on the ordered side), while the high-T region (II) displays 'non-Fermi-liquid' behaviour. The crossovers on either side of II, and the spin-glass phase boundary $T_c(r)$, all scale as $T \sim |r|^{z\nu/(1+\theta_u \nu)}$; the boundary between Ia and Ib obeys $T \sim r^{z\nu}$. The mean-field values of these exponents are $z = 4$, $\nu = 1/4$, and $\theta_u = 2$. The shaded region has classical critical fluctuations described by theories of the type discussed in reference [1].

In the following section we will describe solutions of infinite-range models of the above phases. The insights from these solutions will be used to attack realistic models with short-range interactions in subsequent sections.

3. Infinite-range models

We describe three models, which address different aspects of the phase diagram in figure 1.

3.1. Insulating Heisenberg spins

This subsection reviews the results of reference [13].

We consider the Hamiltonian H with $t_{ij} = 0$ and H_{int} constructed so that the system has exactly one electron per site. The ground state is therefore necessarily insulating, and we are considering a model of the IQP and ISG phases. The exchange interactions J_{ij} are isotropic in spin space and are independent random variables with $\overline{J_{ij}} = 0$ and $\overline{J_{ij}^2} = J_0^2/N_s$, where N_s is the total number of sites. As the mean square value of J_{ij} is independent of $|i - j|$, the model has infinite-range interactions, and each interaction is of order $1/\sqrt{N_s}$.

Even this simple model is, however, not solvable. We need to consider a generalization of the symmetry of the model from SU(2) to SU(N) (N counts the number of spin components of each electron), and also consider the dependence on the 'length' of the spin at each site (labelled by an integer n_b). We then have a family of models labelled by the two integers N, n_b and the familiar spin-1/2 Heisenberg model corresponds to $N = 2$, $n_b = 1$. It has been shown that the infinite-range model is at least partially solvable in the limit $N \to \infty$, $n_b \to \infty$ but with n_b/N fixed at an arbitrary value, and also in the limit $N \to \infty$, n_b fixed.

For N large, the model is in the ISG phase for $n_b/N > \kappa_c$, where κ_c is a numerical constant whose value is not precisely known. In this phase we have

$$\lim_{\tau\to\infty} \overline{\langle S_i(0)S_i(\tau)\rangle} = q_{EA} \neq 0 \tag{6}$$

where τ is imaginary time, and q_{EA} the Edwards–Anderson order parameter. The nature of the approach of the two-point spin correlator to q_{EA} at large τ, and the manner in which q_{EA} vanishes as n_b/N approaches κ_c from above at $T = 0$ have not been determined.

The IQP phase appears for $n_b/N < \kappa_c$, and its properties have been determined a little more explicitly. We now have

$$\overline{\langle S_i(0)S_i(\tau)\rangle} \sim \frac{1}{\tau} \tag{7}$$

for large τ at $T = 0$. The decay of the correlator is quite slow, and as a result, the local dynamic linear spin susceptibility, $\chi_L(\omega)$, diverges logarithmically as the frequency, ω, approaches zero:

$$\chi_L(\omega) \sim \ln\left(\frac{1}{|\omega|}\right) + \mathrm{i}\frac{\pi}{2}\mathrm{sgn}(\omega). \tag{8}$$

In the present model, each spin has the option of forming singlet bonds with a very large number of partners, and the diverging local susceptibility of the IQP phase appears to be due to strong resonance between different pairings.

For comparison with the other infinite-range models considered below, we note that the local spectrum on each site consists of a single doubly degenerate level of an up or a down spin, which are then coupled together by the inter-site exchange interaction. As we will see shortly, this local degeneracy is intimately linked with the diverging local susceptibility of the present model.

3.2. Spins in a metal

This subsection reviews the results of references [9, 10].

We now consider the Hamiltonian H with *both* t_{ij} and J_{ij} independent, Gaussian, random variables, with mean square values independent of i, j. The couplings in H_{int} are chosen so that the ground state is metallic, and therefore produces a mean-field theory of

the MSG and MQP phases, and of the quantum phase transition between them. Unlike the model of subsection 3.1, we have available an essentially exact solution of the low-energy properties of the present model, including that of the critical properties of the MSG–MQP transition, and of the finite-T crossovers.

We will limit our discussion here to $T = 0$; non-zero T will be discussed later in the paper. In the MQP (or disordered Fermi-liquid) phase of this model we have

$$\overline{\langle S_i(0)S_i(\tau)\rangle} \sim \frac{1}{\tau^2} \tag{9}$$

for large τ. This $1/\tau^2$ decay of spin correlations is characteristic of that found in any Fermi liquid. This is perhaps clearer in the Fourier transform to the dynamic local susceptibility, which has the linear form

$$\chi_L''(\omega) \sim \omega \tag{10}$$

of the particle–hole continuum. As one approaches the transition to the MSG phase, the linear form holds only for very small ω, and the dynamic susceptibility is described by the crossover function

$$\chi_L''(\omega) \sim \frac{\omega}{\sqrt{\Delta + \sqrt{\omega^2 + \Delta^2}}}. \tag{11}$$

The energy $\Delta \sim r$ (recall that r is the tuning parameter to the spin-glass transition) is the crossover scale separating Fermi-liquid behaviour for $\omega \ll \Delta$, where (10) holds, to non-Fermi-liquid behaviour for $\omega \gg \Delta$ where $\chi_L''(\omega) \sim \mathrm{sgn}(\omega)\sqrt{\omega}$. This non-Fermi-liquid behaviour holds at all frequencies at the $\Delta = 0$ critical point; in imaginary time the critical spin correlator behaves as

$$\overline{\langle S_i(0)S_i(\tau)\rangle} \sim \frac{1}{\tau^{3/2}}. \tag{12}$$

For $r < 0$, the system is in the MSG phase. We now have

$$\overline{\langle S_i(0)S_i(\tau)\rangle} \sim q_{EA} + \frac{c}{\tau^{3/2}} \tag{13}$$

where c is some constant, and the Edwards–Anderson order parameter vanishes as $q_{EA} \sim r$, as one approaches the critical point to the MQP phase. The entire structure of the Parisi spin-glass order parameter [1] has also been determined [11, 9]: the results closely parallel those of the classical system [1] with replica-symmetry-breaking effects vanishing as $T \to 0$ everywhere in the spin-glass phase.

Finally, it is useful to compare the $1/\tau^2$ decay of correlations in the MQP phase with the $1/\tau$ decay found in subsection 3.1 for the IQP phase. We may interpret this faster decay as a consequence of the reduced local degeneracy of each site. Each spin is coupled to a metallic fermionic bath, which, loosely speaking, lifts the double degeneracy on each site at asymptotically low energies [14].

3.3. Paired spins in an insulator

This is a rather artificial model in the present context, and we discuss it only because it is one of the simplest of the infinite-range models, and closely related models were the first to be solved exactly [15, 16, 11]. Insights gained from their solution were then easily transferred [9, 10] to the metallic case already described.

Consider a random Heisenberg magnet with a natural pairing between the spins described by the Hamiltonian H_p:

$$H_p = \sum_i J_{pi} S_{i1} S_{i2} + \sum_{i<j} \sum_{a,b=1}^{2} J_{ijab} S_{ia} S_{jb}. \tag{14}$$

On each site, i, we now have a pair of spins S_{i1} and S_{i2}, and this pair interacts with an antiferromagnetic exchange $J_{pi} > 0$. The J_{pi} are independent random variables, but they are constrained to be positive, and have a mean value of order unity. The couplings between spins on different sites is however similar to that in H: the J_{ijab} are independent Gaussian random variables with zero mean, and a root mean square value of order $1/\sqrt{N_s}$.

The key property of this model is in the nature of the local spectrum at each site, without including the consequences of the J_{ijab}. The ground state is a non-degenerate singlet and it is separated by a gap, J_{pi}, from the excited triplet state. The local degeneracy referred to in earlier subsections has now been completely lifted. It is this feature which makes the solution of this model relatively straightforward. A similar non-degenerate local ground state, and a gap to the lowest excited state, is also found in spin-glass models of quantum rotors [16] and Ising spins in a transverse field [15]; the properties of these models are essentially identical to those described here.

The local spin correlations in the IQP phase now decay exponentially in the infinite-range model:

$$\overline{\langle S_i(0) S_i(\tau)\rangle} \sim \mathrm{e}^{-\Delta\tau} \tag{15}$$

where Δ is an energy scale which vanishes at the transition to the ISG phase. The exponential decay is actually an artifact of the infinite-range model, and Griffiths effects in finite-range models lead to a stretched exponential contribution $\sim \exp(-c'\sqrt{\tau})$, which dominates at long enough times. For the local dynamic susceptibility, these statements mean that there is an energy gap Δ in the IQP phase of the infinite-range model; Griffiths effects induce a weak subgap absorption of order $\exp(-c''/|\omega|)$ in models with finite-range interactions. The gap of the infinite-range model $\Delta \sim r/\ln(1/r)$ as one approaches the critical point at $r = 0$.

Notice the faster decay of correlations in the IQP phase of the present model, as compared to those discussed earlier. This is a consequence of the complete lifting of the on-site degeneracy.

Near the critical point, the crossover function analogous to (11) is

$$\chi_L''(\omega) \sim \mathrm{sgn}(\omega)\sqrt{\omega^2 - \Delta^2}\,\theta(|\omega| - \Delta). \tag{16}$$

So, at the critical point $\Delta = 0$, we have $\chi_L''(\omega) \sim \omega$, and spin correlations decay as $1/\tau^2$. In the spin-glass phase, the analogue of (13) is

$$\overline{\langle S_i(0) S_i(\tau)\rangle} \sim q_{EA} + \frac{c}{\tau^2}. \tag{17}$$

Other properties of the spin glass are similar to those described in subsection 3.2.

4. The order parameter and Landau theory

This section reviews the results of references [11] and [9].

For the cases of the paired-spin model of subsection 3.3, and the spins in a metal model of subsection 3.2, it is possible to go beyond the infinite-range model and study the corresponding quantum transitions in systems with short-range interactions. The basic

strategy is similar to that followed in the classical spin-glass case: introduce an order parameter characterizing the important long-time spin correlations, and use insights from the solution of the infinite-range model, and general symmetry considerations, to obtain Landau functionals describing fluctuations in the case with finite-range interactions. This procedure was carried out in reference [11] for the quantum rotor model (whose properties are essentially identical to the paired-spin model of subsection 3.3), and in reference [9] for the metallic spin-glass case. No such extension exists yet for the insulating Heisenberg spin case (subsection 3.1), and its development remains an important open problem.

In the following subsections we will (i) introduce the order parameter for the transition from a quantum spin glass to a paramagnet [11], (ii) obtain Landau functionals for finite-range versions of the models of subsections 3.3 [11] and 3.2 [9], and (iii) show that a simple minimization of these functionals reproduces the properties of the infinite-range models, and describe crossovers for a number of observables. The consequences of fluctuations in finite-range models are discussed in section 5.

4.1. The order parameter

We begin by introducing the order parameter for the quantum phase transition [11]. Recall that for classical spin glasses in the replica formalism, this is a matrix q^{ab}, $a, b = 1, \ldots, n$ are replica indices, and $n \to 0$. The *off-diagonal* components of q^{ab} can be related to the Edwards–Anderson order parameter, q_{EA}, in a somewhat subtle way that we will not go into here [1, 17]. In quantum ($T = 0$) phase transitions, time-dependent fluctuations of the order parameter must be considered (in 'imaginary' Matsubara time τ), and in the spin-glass case it is found that the standard decoupling, analogous to the classical case introducing q^{ab}, leads now to a matrix function of two times [18] which we can consider to be

$$Q^{ab}(x, \tau_1, \tau_2) = \sum_{i \in \mathcal{N}(x)} S_i^a(\tau_1) S_i^b(\tau_2) \tag{18}$$

where $\mathcal{N}(x)$ is a coarse-graining region in the neighbourhood of x. From the set-up of the replica formalism it is clear that

$$\overline{\langle S_i(0) S_i(\tau) \rangle} = \lim_{n \to 0} \frac{1}{n} \sum_a \left\langle\!\left\langle Q^{aa}(x, \tau_1 = 0, \tau_2 = \tau) \right\rangle\!\right\rangle \tag{19}$$

$$q_{EA} = \lim_{\tau \to \infty} \lim_{n \to 0} \frac{1}{n} \sum_a \left\langle\!\left\langle Q^{aa}(x, \tau_1 = 0, \tau_2 = \tau) \right\rangle\!\right\rangle \tag{20}$$

relating q_{EA} to the replica *diagonal* components of Q. We have introduced above double angular brackets to represent averages taken with the translationally invariant replica action (recall that single angular brackets represent thermal/quantum averages for a fixed realization of randomness, and overlines represent averages over randomness). Notice that the fluctuating field Q is in general a function of two separate times τ_1 and τ_2; however, the expectation value of its replica diagonal components can only be a function of the time difference $\tau_1 - \tau_2$. Further, the expectation value of the replica off-diagonal components of Q is independent of both τ_1 and τ_2 [16], and has a structure very similar to that of the classical order parameter q^{ab}. One can therefore also obtain q_{EA} from the replica off-diagonal components of Q, as noted above for q^{ab} [1, 17]. Let us also note for completeness that, unlike in the quantum case, the replica diagonal components of the classical order parameter q^{ab} are usually constrained to be unity [1], and contain no useful information.

The order parameter that we will use is $Q^{ab}(x, \tau_1, \tau_2)$, which is a matrix in a replica space and depends on the spatial coordinate x and two times τ_1, τ_2. However, a little

thought shows that this function contains too much information. The important degrees of freedom, for which one can hope to make general and universal statements, are the long-time spin correlations with $|\tau_1 - \tau_2| \gg \tau_m$, where τ_m is a microscopic time like an inverse of a typical exchange constant. As presented, the function Q contains information not only on the interesting long-time correlations, but also on the uninteresting time range with $|\tau_1 - \tau_2|$ smaller than or of the order of τ_m. The correlations in the latter range are surely model dependent and cannot be part of any general Landau action. We shall separate out this uninteresting part of Q by performing the shift

$$Q^{ab}(x, \tau_1, \tau_2) \to Q^{ab}(x, \tau_1, \tau_2) - C\delta^{ab}\delta(\tau_1 - \tau_2) \tag{21}$$

where C is a constant, and the delta function $\delta(\tau_1 - \tau_2)$ is a schematic form for a function which decays rapidly to zero on a scale τ_m. The value of C will be adjusted so that the resulting Q contains only the interesting long-time physics: we will see later how this can be done in a relatively straightforward manner. The alert reader may recognize some similarity between the above procedure, and Fisher's analysis [19] of the Yang–Lee edge problem. In that case, too, the order parameter contains an uninteresting non-critical piece which has to be shifted away; we will see below that there many other similarities between the Yang–Lee edge and quantum spin-glass problems.

4.2. The action functional

The action functional can be derived by explicit computations on microscopic models or deduced directly from general arguments which have been discussed in some detail in reference [11]. Apart from a single non-local term present in the metallic case [9] (see below), the remaining important terms are consistent with the general criteria [11] listed below.

(i) The action is an integral over space of a local operator which can be expanded in gradients of powers of Q evaluated at the same position x.

(ii) Q is bilocal (i.e. is a matrix) in time, and each time is associated with one of the two replica indices (see the definition: equation (18)). These 'indices' can appear more than once in a term and are summed over freely subject to the following rules before summations:

  (a) each distinct replica index appears an even number of times [1];

  (b) repetition of a time 'index' corresponds to quantum mechanical interaction of spins, which must be local in time, and accordingly can be expanded as terms with times set equal plus the same with additional derivatives; it occurs when the corresponding replica indices are the same, and only then.

We now present all the terms which a subsequent renormalization group analysis tells us are important near the quantum critical point. This is only a small subset of the terms allowed by the above criteria.

A crucial term is that linear in the order parameter Q. This term encodes the local, on-site physics of the spin-glass model. To the order that we shall consider, this is the only term which distinguishes between the finite-range analogues of the models of subsections 3.2 and 3.3. For the paired-spin model of subsection 3.3 we find the linear term [11]

$$\frac{1}{\kappa t}\int \mathrm{d}^d x\ \mathrm{d}\tau\ \sum_a \left[\frac{\partial}{\partial\tau_1}\frac{\partial}{\partial\tau_2} + \widetilde{r}\right] Q^{aa}(x, \tau_1, \tau_2)\Big|_{\tau_1=\tau_2=\tau}. \tag{22}$$

The gap in the on-site spectrum for this model tells us that it is valid to expand the linear term in derivatives of τ, and the above contains the leading-order contributions. The coupling

$\widetilde{r}$ will be seen below to be the critical tuning parameter for the transition from the spin glass to the paramagnet (it is related to the parameter r, introduced earlier, by an additive constant). There is an overall factor of $1/\kappa t$ in front of this term; we have written this factor as a product of two coupling constants, κ and t, for technical reasons [11] that we will not discuss here. Turning to the metallic model (subsection 3.2) we find, instead, the linear term [9]

$$\frac{1}{\kappa t}\int \mathrm{d}^d x\ \left\{\int \mathrm{d}\tau\ \sum_a r\, Q^{aa}(x,\tau,\tau) - \frac{1}{\pi}\int \mathrm{d}\tau_1\ \mathrm{d}\tau_2\ \sum_a \frac{Q^{aa}(x,\tau_1,\tau_2)}{(\tau_1-\tau_2)^2}\right\}. \tag{23}$$

Now the coupling of the local spin degree of freedom to the itinerant quasiparticles has introduced a long-range $1/\tau^2$ interaction in imaginary time: this is clearly related to the result (9). A term with two time derivatives, like that in (22), is also permitted, but it is not as important at long times.

The remaining terms presented here apply to both the insulating paired spins and spins in a metal model.

There is a quadratic gradient term

$$\frac{1}{2t}\int \mathrm{d}^d x\ \mathrm{d}\tau_1\ \mathrm{d}\tau_2\ \sum_{a,b}\left[\boldsymbol{\nabla} Q^{ab}(x,\tau_1,\tau_2)\right]^2 \tag{24}$$

which is responsible for the development of spatial correlations in the spin-glass order. Clearly, such a term is absent in the infinite-range case, and is special to the more realistic short-range case. A quadratic term without gradients

$$\int \mathrm{d}^d x\ \mathrm{d}\tau_1\ \mathrm{d}\tau_2\ \sum_{a,b}\left[Q^{ab}_{\mu\nu}(x,\tau_1,\tau_2)\right]^2 \tag{25}$$

is also allowed by the general criteria, but we choose to tune its coefficient to zero by using the freedom in (21). As will become clear in subsection 4.3, this criterion is identical to requiring the absence of uninteresting short-time behaviour in Q. Notice again the formal similarity to the theory of the Yang–Lee edge [19], where setting the coefficient of a quadratic term to zero was also responsible for removing the uninteresting non-critical part of the order parameter variable.

Next we consider cubic non-linearities, and the most important among the several allowed terms is the one with the maximum number of different time and replica indices:

$$-\frac{\kappa}{3t}\int \mathrm{d}^d x\ \mathrm{d}\tau_1\ \mathrm{d}\tau_2\ \mathrm{d}\tau_3 \sum_{a,b,c} Q^{ab}(x,\tau_1,\tau_2)Q^{bc}(x,\tau_2,\tau_3)Q^{ca}(x,\tau_3,\tau_1). \tag{26}$$

This term accounts for non-linearities induced solely by disorder fluctuations.

Of the terms with fewer than the maximum allowed number of time indices at a given order, the most important one is the one at quadratic order:

$$\frac{u}{2t}\int \mathrm{d}^d x\ \mathrm{d}\tau\ \sum_a u\ Q^{aa}(x,\tau,\tau)Q^{aa}(x,\tau,\tau). \tag{27}$$

We have ignored vector spin indices (μ,ν) here, and if these were accounted for, we would have found two separate terms with the same replica and time integration structure as (27) [11]; however, the additional term does not significantly modify the physics, and we will ignore it here. The coupling u is the only one responsible for quantum mechanical interactions between the spins, and as a consequence, all of the time and replica indices in (27) are the same.

Lastly we have a final quadratic term

$$-\frac{1}{2t^2}\int \mathrm{d}^d x \int \mathrm{d}\tau_1\ \mathrm{d}\tau_2 \sum_{a,b} Q^{aa}(x,\tau_1,\tau_1)Q^{bb}(x,\tau_2,\tau_2) \tag{28}$$

which accounts for the spatial fluctuation in the position of the paramagnet–spin-glass transition. Recall that the linear coupling $\widetilde{r}$ was the control parameter for this transition, and a term like (28) is obtained by allowing for Gaussian fluctuations in $\widetilde{r}$, about its mean value, from point to point in space. It will turn out that (28) plays no role in the mean-field analysis in the following subsection. However, it is essential to include (28) for a proper theory of the fluctuations, and its effects are responsible for ensuring that the correlation length exponent, ν, satisfies the inequality [20] $\nu > 2/d$.

To summarize this subsection, the action functional for the paired-spin model with short-range interactions is (22) + (24) + (26) + (27) + (28), while that for the spins in a metal case is (23) + (24) + (26) + (27) + (28). Notice that the two differ only in the form of the linear term, which is (22) for the paired-spin case, and (23) for the metallic case.

4.3. Mean-field theory

We will limit our discussion in this subsection to the metallic case. We will review the mean-field theory for the MQP phase [9, 10] and identify the position of its instability to the MSG phase. A discussion of the solution within the MSG phase will not be presented here, and appears elsewhere [9].

We Fourier transform from imaginary time to Matsubara frequencies by expressing the action in terms of

$$Q^{ab}(x,\omega_1,\omega_2) = \int_0^{1/T} \mathrm{d}\tau_1\ \mathrm{d}\tau_2\ Q^{ab}(x,\tau_1,\tau_2)\mathrm{e}^{-\mathrm{i}(\omega_1\tau_1+\omega_2\tau_2)} \tag{29}$$

where we are using units in which $\hbar = k_B = 1$, and the frequencies, ω_1, ω_2 are quantized in integer multiples of $2\pi T$. Then, we make an *ansatz* for the mean-field value of Q which is x-independent, and dependent only on $\tau_1 - \tau_2$; within the MQP phase this takes the form

$$Q^{ab}(x,\omega_1,\omega_2) = (\delta^{ab}\delta_{\omega_1+\omega_2,0}/T)\chi_L(\mathrm{i}\omega_1) \tag{30}$$

where we have used (20) to identify the right-hand side as the local dynamic susceptibility. Inserting (30) into the action for the metallic case in subsection 4.2, we get for the free energy per unit volume $\mathcal{F}/n$ (as usual [1], $\mathcal{F}/n$ represents the physical disorder-averaged free energy)

$$\frac{\mathcal{F}}{n} = \frac{T}{t}\sum_{\omega}\left[\frac{|\omega|+\widetilde{r}}{\kappa}\chi_L(\mathrm{i}\omega) - \frac{\kappa}{3}\chi_L^3(\mathrm{i}\omega)\right] + \frac{u}{2t}\left[T\sum_{\omega}\chi_L(\mathrm{i}\omega)\right]^2. \tag{31}$$

Notice that the coupling $1/t$ appears only as a prefactor in front of the total free energy, as the contribution of the $1/t^2$ term (28) vanishes in the replica limit $n \to 0$. The value of t will therefore play no role in the mean-field theory. We now determine the saddle point of (31) with respect to variations in the whole function $\chi_L(\mathrm{i}\omega)$, and find the solution

$$\chi_L(\mathrm{i}\omega) = -\frac{1}{\kappa}\sqrt{|\omega|+\Delta} \tag{32}$$

where the energy scale Δ is determined by the solution of the equation

$$\Delta = \widetilde{r} - uT\sum_{\omega}\sqrt{|\omega|+\Delta} \tag{33}$$

Taking the imaginary part of the analytic continuation of (32) to real frequencies, we get

$$\chi_L''(\omega) = \frac{1}{\kappa\sqrt{2}} \frac{\omega}{\sqrt{\Delta + \sqrt{\omega^2 + \Delta^2}}} \tag{34}$$

which was also the result (11) for the infinite-range model. Inserting the solution for χ_L back into (31), and using (33), we get for the free-energy density

$$\frac{\mathcal{F}}{n} = -\frac{1}{\kappa^2 t}\left[\frac{2T}{3}\sum_{\omega}(|\omega| + \Delta)^{3/2} + \frac{u}{2}(T\sum_{\omega}\sqrt{|\omega| + \Delta})^2\right]. \tag{35}$$

The equations (33), (34), (35) are key results [9, 10], from which our mean-field predictions for physical observables will follow. Despite their apparent simplicity, these results contain a great deal of structure, and a fairly careful and non-trivial analysis is required to extract the universal information contained within them.

First, it is easy to note that there is no sensible solution (with $\Delta > 0$) of (33) at $T = 0$ for $\widetilde{r} < \widetilde{r}_c$ where

$$\widetilde{r}_c = u\int \frac{\mathrm{d}\omega}{2\pi}\ \sqrt{|\omega|} \approx \frac{2\Lambda_\omega^{3/2}}{3\pi} \tag{36}$$

where Λ_ω is an upper cut-off in frequency. Clearly the system is in the MSG phase for $T = 0$, $\widetilde{r} < \widetilde{r}_c$, and a separate *ansatz* for Q is necessary there, as discussed elsewhere [9]. Let us now define

$$r \equiv \widetilde{r} - \widetilde{r}_c \tag{37}$$

so that the quantum critical point is at $T = 0$, $r = 0$. In the vicinity of this point, our action constitutes a continuum quantum field theory (CQFT) describing the physics of the system at all energy scales significantly smaller than Λ_ω. The 'universal' properties of the system are the correlators of this CQFT, and they apply therefore for $r, T \ll \Lambda_\omega$, a condition that we assume in our analysis below. It is also natural to assume that the microscopic coupling $u \sim \Lambda_\omega^{-1/2}$. We shall, however, make no assumptions on the relative magnitudes of r and T.

Let us now examine the solution of (33) under the conditions noted above. Clearly, we have from (33) and (37) that

$$\Delta + uT\sqrt{\Delta} = r - u\left(T\sum_{\omega\neq 0}\sqrt{|\omega| + \Delta} - \int \frac{\mathrm{d}\omega}{2\pi}\ \sqrt{|\omega|}\right). \tag{38}$$

We have chosen to move the $\omega = 0$ term in the frequency summation from the right-hand to the left-hand side. This permits us to replace the Δ on the right-hand side by its zeroth-order result in an expansion in u, as all neglected terms can be shown to be less singular as one approaches the critical point. After doing this, we further manipulate (38) into

$$\begin{aligned}\Delta + uT\sqrt{\Delta} = r + uT\sqrt{r} - u\left(T\sum_{\omega}\sqrt{|\omega| + r} - \int \frac{\mathrm{d}\omega}{2\pi}\ \sqrt{|\omega| + r}\right) \\ - u\int \frac{\mathrm{d}\omega}{2\pi}\left(\sqrt{|\omega| + r} - \sqrt{|\omega|} - \frac{r}{2\sqrt{|\omega|}}\right) - u\int \frac{r}{2\sqrt{|\omega|}}.\end{aligned} \tag{39}$$

In the first term on the right-hand side, the objective has been to always subtract from the summation over Matsubara frequencies of any function the integration of precisely the same function; the difference is then strongly convergent in the ultraviolet, and such a procedure leads naturally to finite-temperature crossover functions [21]. The second term also has a subtraction to make it convergent in the ultraviolet. We will now manipulate (39) into a

form where it is evident that Δ is analytic as a function of r at $r = 0$ for $T \neq 0$. There is a thermodynamic singularity at the quantum critical point $T = 0$, $r = 0$, but this must disappear at $r = 0$ for any non-zero T [21] (see figure 2). We use the identity

$$\int_0^\infty \sqrt{s}\ \mathrm{d}s\ \left(\frac{1}{s+a} - \frac{1}{s+b}\right) = \pi(\sqrt{b} - \sqrt{a}) \tag{40}$$

to rewrite (39) as

$$\begin{aligned}\Delta + uT\sqrt{\Delta} = {} & r\left(1 - \frac{u\Lambda_\omega^{1/2}}{\pi}\right) + uT\sqrt{r} \\ & + \frac{u}{\pi}\int_0^\infty \sqrt{s}\ \mathrm{d}s\ \left(T\sum_\omega \frac{1}{s+|\omega|+r} - \int \frac{\mathrm{d}\omega}{2\pi}\ \frac{1}{s+|\omega|+r}\right) \\ & + \frac{u}{\pi}\int_0^\infty \sqrt{s}\ \mathrm{d}s\ \int \frac{\mathrm{d}\omega}{2\pi}\ \left(\frac{1}{s+|\omega|+r} - \frac{1}{s+|\omega|} + \frac{r}{(s+|\omega|)^2}\right).\end{aligned} \tag{41}$$

We now evaluate the frequency summation by expressing it in terms of the digamma function ψ, and perform all frequency integrals exactly. After some elementary manipulations (including use of the identity $\psi(s+1) = \psi(s) + 1/s$), we obtain our final result for Δ, in the form of a solvable quadratic equation for $\sqrt{\Delta}$:

$$\Delta + uT\sqrt{\Delta} = r\left(1 - \frac{u\Lambda_\omega^{1/2}}{\pi}\right) + uT^{3/2}\Phi\left(\frac{r}{T}\right) \tag{42}$$

where the universal crossover function $\Phi(y)$ is given by

$$\Phi(y) = \frac{1}{\pi^2}\int_0^\infty \sqrt{s}\ \mathrm{d}s\ \left[\log\left(\frac{s}{2\pi}\right) - \psi\left(1 + \frac{s+y}{2\pi}\right) + \frac{\pi+y}{s}\right]. \tag{43}$$

The above expression for $\Phi(y)$ is clearly analytic for all $y \geqslant 0$, including $y = 0$, as required from general thermodynamic considerations [21]. Indeed, we can use the above result even for $y < 0$ until we hit the first singularity at $y = -2\pi$, which is associated with singularity of the digamma function $\psi(s)$ at $s = 0$. However, this singularity is of no physical consequence, as it occurs within the spin-glass phase (figure 2), where the above solution is not valid; as shown below, the transition to the spin-glass phase occurs for $y \sim -uT^{1/2}$ which is well above -2π. It is useful to have the following limiting results, which follow from (43), for our subsequent analysis:

$$\Phi(y) = \begin{cases} \sqrt{1/2\pi}\,\zeta(3/2) + \mathcal{O}(y) & y \to 0 \\ (2/3\pi)y^{3/2} + y^{1/2} + (\pi/6)y^{-1/2} + \mathcal{O}(y^{-3/2}) & y \to \infty. \end{cases} \tag{44}$$

The expression (34), combined with the results (42) and (43) completely specify the r- and T-dependence of the dynamic susceptibility in the MQP phase, and allow us to obtain the phase diagram shown in figure 2. The crossovers shown are properties of the CQFT characterizing the quantum critical point. We present below explicit results for the crossover functions of a number of observables within the mean-field theory. A more general scaling interpretation will be given in section 5.

Before describing the crossovers, we note that the full line in figure 2 denotes the boundary of the paramagnetic phase at $r = r_c(T)$ (or $T = T_c(r)$). This is the only line of thermodynamic phase transitions, and its location is determined by the condition $\Delta = 0$, which gives us

$$r_c(T) = -u\Phi(0)T^{3/2} \qquad \text{or} \qquad T_c(r) = (-r/u\Phi(0))^{2/3}. \tag{45}$$

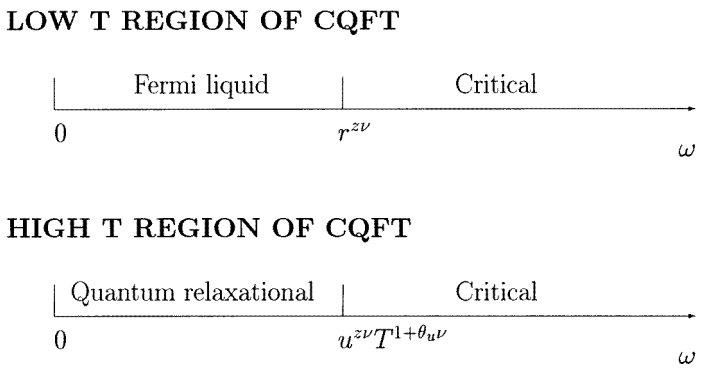

Figure 3. Crossovers as a function of frequency, ω, in the regions of figure 2. The low-T region is on the paramagnetic side ($r > 0$).

The different regimes in figure 2 can be divided into two classes determined by whether T is 'low' or 'high'. There are two low-T regimes, one for $r > 0$, and the other for $r < 0$; these regions display properties of the non-critical ground states, which were reviewed in section 2. More novel is the high-T region, where the most important energy scale is set by T, and 'non-Fermi-liquid' effects associated with the critical ground state occur. We now describe the regimes in more detail, in turn.

(I) *The low-T region above the MQP ground state, $T < (r/u)^{2/3}$.* This is the 'Fermi-liquid' region, where the leading contribution to Δ is its $T = 0$ value $\Delta(T) \sim \Delta(0) = r$. The leading temperature-dependent correction to Δ is however different in two subregions. In the lowest-T region, Ia, $T < r$, we have the Fermi-liquid T^2 power law

$$\Delta(T) - \Delta(0) = \frac{u\pi T^2}{6\sqrt{r}} \qquad \text{region Ia.} \tag{46}$$

At higher temperatures, in region Ib, $r < T < (r/u)^{2/3}$, we have an anomalous temperature dependence

$$\Delta(T) - \Delta(0) = u\Phi(0)T^{3/2} \qquad \text{regions Ib and II.} \tag{47}$$

It is also interesting to consider the properties of region I as a function of observation frequency, ω, as sketched in figure 3. At large frequencies, $\omega \gg r$, the local dynamic susceptibility behaves like $\chi_L'' \sim \mathrm{sgn}(\omega)\sqrt{|\omega|}$, which is the spectrum of critical fluctuations; at the $T = 0$, $r = 0$ critical point, this spectrum is present at all frequencies. At low frequencies, $\omega \ll r$, there is a crossover (figure 3) to the characteristic Fermi-liquid spectrum of local spin fluctuations $\chi_L'' \sim \omega/\sqrt{r}$.

(II) *The high-T region, $T > (|r|/u)^{2/3}$.* This is the 'non-Fermi-liquid' region, where temperature-dependent contributions to Δ dominate over those due to the deviation of the coupling r from its critical point, $r = 0$. Therefore thermal effects are dominant, and the system behaves as if its microscopic couplings are at those of the critical ground state. The T-dependence in (47) continues to hold, as we have already noted, with the leading contribution now being $\Delta \approx u\Phi(0)T^{3/2}$. As in (I), it is useful to consider properties of this region as a function of ω (figure 3). For large ω ($\omega \gg uT^{3/2}$) we again have the critical behaviour $\chi_L'' \sim \mathrm{sgn}(\omega)\sqrt{|\omega|}$; this critical behaviour is present at large enough ω in all of the regions of the phase diagram. At small ω ($\omega \ll uT^{3/2}$), thermal fluctuations quench the critical fluctuations, and we have relaxational behaviour with $\chi_L'' \sim \omega/u^{1/2}T^{3/4}$.

(III) *The low-T region above the MSG ground state, $T < (-r/u)^{2/3}$.* Effects due to the formation of a static moment are now paramount. As one approaches the spin-glass boundary (45) from above, the system enters a region of purely classical thermal fluctuations, $|T - T_c(r)| \ll u^{2/3} T_c^{4/3}(r)$ (shown shaded in figure 2) where

$$\Delta = \left(\frac{r - r_c(T)}{Tu} \right)^2 . \tag{48}$$

Notice that Δ depends on the square of the distance from the finite-T classical phase transition line, in contrast to its linear dependence, along $T = 0$, on the deviation from the quantum critical point at $r = 0$.

We have now completed a presentation of the mean-field predictions for the finite-T crossovers near the quantum critical point (figure 2), and for the explicit crossover functions for the frequency-dependent local dynamic susceptibility (figure 3 and equations (34), (42), (43)). We will now consider the implications of our results for a number of other experimental observables.

4.3.1. Nuclear relaxation. This was considered in reference [10]. The $1/T_1$ relaxation rate of nuclei coupled to the electronic spins by a hyperfine coupling is given by the low-frequency limit of the local dynamic susceptibility. We have

$$\frac{1}{T_1 T} = A^2 \lim_{\omega \to 0} \frac{\chi_L''(\omega)}{\omega} = \frac{A^2}{2\kappa\sqrt{\Delta}} \tag{49}$$

where A is determined by the hyperfine coupling. The crossover function for $1/T_1$ now follows from that for Δ in (42), (43). In particular, in region (II), $1/T_1 \sim T^{1/4}$ [10].

4.3.2. Uniform linear susceptibility. In the presence of a uniform magnetic field, H, the action acquires the term [9]

$$-\frac{g}{2t} \int \mathrm{d}^d x \; \mathrm{d}\tau_1 \; \mathrm{d}\tau_2 \; \sum_{ab\mu\nu} Q^{ab}_{\mu\nu}(x, \tau_1, \tau_2) H_\mu H_\nu \tag{50}$$

where μ, ν are spin indices. There are a number of additional terms involving H [9], but their linear response is always weaker than that due to (50). Taking the second derivative of the free energy with respect to H, we obtain for the uniform linear susceptibility, χ_u [11, 10]:

$$\chi_u = \chi_b - \frac{g}{t\kappa}\sqrt{\Delta} \tag{51}$$

where χ_b is the T, r- independent background contribution of the fermions that have been integrated out. The crossover function for χ_u now follows, as for $1/T_1$, from that for Δ.

4.3.3. Nonlinear susceptibility. The non-linear response to (50) was computed in reference [11]. The nonlinear susceptibility was found to be

$$\chi_{nl} = \frac{u g^2}{4t} \frac{1}{\Delta} \tag{52}$$

and its crossover function again follows from that for Δ. Notice that χ_{nl} is proportional to the quantum mechanical interaction u, and would vanish in a theory with terms associated only with disorder fluctuations.

4.3.4. The free energy and specific heat. The result for the free energy was given in (35), and it needs to be evaluated along the lines of the analysis carried out above for the crossover function determining Δ. The specific heat then follows via the usual thermodynamic relation. After performing the necessary frequency summations and integrations, we obtained the crossover function for the free-energy density:

$$\frac{\mathcal{F}(T,r)-\mathcal{F}(T=0,r=0)}{n} = -\frac{1}{\kappa^2 t}\left[\frac{2r\Lambda_\omega^{3/2}}{3\pi}+T^{5/2}\Phi_{\mathcal{F}}\left(\frac{\Delta}{T}\right)+\frac{\Lambda_\omega\Delta^2}{2\pi}+\frac{(\Delta-r)^2}{2u}-\frac{4\Delta^{5/2}}{15\pi}\right] \tag{53}$$

where

$$\Phi_{\mathcal{F}}(y) = -\frac{2\sqrt{2}}{3\pi}\int_0^\infty \frac{\mathrm{d}\Omega}{\mathrm{e}^\Omega-1}\,\frac{\Omega(2y+\sqrt{\Omega^2+y^2})}{\sqrt{y+\sqrt{\Omega^2+y^2}}}. \tag{54}$$

This result for $\mathcal{F}$ includes non-singular contributions, smooth in r, which form a background to the singular critical contributions. In region (II), the most singular term is the one proportional to $\Phi_{\mathcal{F}}$, and yields a specific heat, C_v [10]:

$$\frac{C_v}{T} = \gamma_b - \frac{\zeta(5/2)}{\sqrt{2\pi}\kappa^2 t}\sqrt{T} \tag{55}$$

where γ_b is a background contribution.

4.3.5. Charge transport. The consequences of the order parameter fluctuations for charge transport were explored by Sengupta and Georges [10]. The quasiparticles are assumed to carry both charge and spin, and they scatter off the spin fluctuations via an exchange coupling. In the Born approximation, this leads to a contribution to the quasiparticle relaxation rate, $1/\tau_{qp}$:

$$\frac{1}{\tau_{qp}} \propto \int_0^\infty \frac{\mathrm{d}\Omega}{\sinh(\Omega/T)}\,\frac{\Omega}{\sqrt{\Delta+\sqrt{\Omega^2+\Delta^2}}} \tag{56}$$

whose T- and r-dependence follows from that of Δ. In region (II), $1/\tau_{qp} \sim T^{3/2}$.

5. Fluctuations and scaling analysis

Fluctuations about the mean-field theory just described have been discussed in some detail in references [11, 9], and we will be quite brief here. As in subsection 4.3, we will also restrict all of our discussion to the metallic spin-glass case.

The structure of the corrections can be understood by examining the behaviour of the action under the renormalization group transformation

$$x \to x\mathrm{e}^{-\ell} \qquad \tau \to \tau \mathrm{e}^{-z\ell}. \tag{57}$$

The mean-field theory has the dynamic exponent $z = 4$.

The system is tuned across the transition by the control parameter r, and by the definition of the correlation length exponent, ν, it obeys

$$\frac{\mathrm{d}r}{\mathrm{d}\ell} = \frac{1}{\nu}r + \cdots. \tag{58}$$

In mean-field theory we have $\nu = 1/4$.

The quantum mechanical interaction, u, obeys for weak coupling

$$\frac{\mathrm{d}u}{\mathrm{d}\ell} = -\theta_u u \tag{59}$$

with $\theta_u = 2$. So the mean-field theory in fact corresponds to a fixed point with $u^* = 0$, and all u-dependent corrections are, in some sense, corrections to scaling. It is essential to include such corrections, as none of the remaining couplings involve quantum mechanical interactions between the order parameter modes, and therefore lead to contributions insensitive to the value of T.

The parameter t controls fluctuations of disorder, and for weak coupling its renormalization group equation is

$$\frac{\mathrm{d}t}{\mathrm{d}\ell} = -\theta t \tag{60}$$

with $\theta = 2$. The value of t was immaterial in the mean-field theory, and it might appear from the flow (60) that we can set $t = 0$ in the analysis of the fluctuations. This is not strictly correct, as many quantities have a singular dependence on t as $t \to 0$. As a result, t behaves like a 'dangerously irrelevant' variable and modifies 'hyperscaling' relations between exponents. These effects are discussed in more detail in references [11, 9], and as they are peripheral to the emphasis here, we will not say more.

Finally, the cubic non-linearity, κ, obeys

$$\frac{\mathrm{d}\kappa}{\mathrm{d}\ell} = \frac{8-d}{2}\kappa + 9\kappa^3. \tag{61}$$

For $d > 8$, there is a stable fixed point at $\kappa = 0$, which describes the mean-field solution discussed in subsection 4.3. However, for the physically interesting region where $d < 8$, this fixed point is unstable and the system has a runaway flow to strong coupling. So we have no systematic way of controlling the corrections due to fluctuations.

Under these circumstances, the best that we can hope to do is to use the insight gained from the mean-field solution to speculate on some reasonable scaling scenarios. Two natural possibilities arise, depending upon whether the fixed-point values of u and other quantum mechanical interactions are all zero (a *static* fixed point) or not (a *dynamic* fixed point). The static fixed point will have a $\theta_u > 0$; more generally θ_u is the negative of the renormalization group eigenvalue of the least irrelevant of the quantum mechanical couplings. Observables sensitive to the order parameter modes will have their T-dependence controlled by the value of θ_u. Dynamic fixed points have non-zero quantum interactions already in the critical theory, and their finite-T crossovers were reviewed recently in reference [22]; they correspond to the $\theta_u = 0$ case of the finite-T behaviours of static fixed points, discussed below.

The remaining discussion summarizes a scaling interpretation of the results of the mean-field theory in terms of a static fixed point; we propose that the behaviour of a generic static fixed point will be similar, but with different numerical values for the exponents. The crossovers are interpreted in terms of the exponents z, ν, θ, θ_u and an order parameter anomalous dimension η. Recall that the mean-field theory has $z = 4$, $\nu = 1/4$, $\theta = 2$, $\theta_u = 2$, and $\eta = 0$. Using arguments presented in reference [9], we can deduce the expected behaviour of all of the phase boundaries in figure 2 at the inaccessible (but presumed static) fixed point, in terms of the above exponents; the results are summarized in the caption to figure 2. Within region II of figure 2, we obtain the following T-dependencies for the

observables considered in the mean-field theory:

$$\begin{aligned}
&\frac{1}{T_1 T} \sim T^{(d-\theta-2-2z+\eta)(1+\theta_u \nu)/2z} \\
&\chi_u \sim T^{(d-\theta-2+\eta)(1+\theta_u \nu)/2z} \\
&\chi_{nl} \sim T^{-(2+z-\eta-\theta_u)(1+\theta_u \nu)/z} \\
&\frac{C_v}{T} \sim T^{(d-z-\theta)/z} \\
&\frac{1}{\tau_{qp}} \sim T^{(d-\theta+2z-2+\eta)/2z}.
\end{aligned} \tag{62}$$

The mean-field results are obtained by using the mean-field exponents and setting $d = 8$.

Reference [9] presented additional speculations on the static fixed point by examining the structure of the perturbation theory of the action of subsection 4.2. It was found that the most singular terms in the perturbation series were identical to those of a much simpler *classical* statistical mechanics problem: that of the Yang–Lee edge in a random Ising ferromagnet. This mapping, and some additional assumptions, led to the exponent relations

$$\begin{aligned}
&z\nu = 1 \\
&\frac{1}{\nu} = \frac{d - \theta + 2 - \eta}{2}.
\end{aligned} \tag{63}$$

As expected, these relations are satisfied by the mean-field theory for the upper critical dimension $d = 8$.

6. Conclusions

It should be clear that much additional work remains to be done, especially with regard to understanding the consequences of disorder-induced fluctuations. Among the issues that could be looked at in future work are the following.

- Is the quantum critical point for the MSG–MQP transition purely static, i.e. does it have no quantum mechanical interactions between the order parameter modes?
- A particular feature of our mappings to static critical points is that all of the exponents and crossovers are insensitive to the number of spin components of the order parameter, M, at least at all fixed points accessible within perturbation theory. The mapping to the random Yang–Lee edge, if correct, would also imply an independence of M. More recently, Senthil and Majumdar [23], have exactly obtained the critical properties of a number of random, insulating, quantum spin chains, and found that the critical exponents are also independent of M. An important open question, then, is that of whether this independence also holds for realistic metallic and insulating quantum spin glasses.
- It would be useful to study the classical, random, Yang–Lee edge problem in more detail. In particular, although this is a non-trivial problem for $d = 2$, the critical theory is expected to be conformally invariant, and progress may be possible using modern methods for such systems.
- While we have a complete mean-field theory for the MSG–MQP transition, there is no such theory for the ISG–IQP transition. The IQP–ISG transition is not understood even in the infinite-range model, and further progress should be possible.

Acknowledgments

We are grateful to our collaborators on the work reviewed here, J Ye and R Oppermann. We thank J Mydosh and T Senthil for valuable comments on the manuscript. This research was supported by the US National Science Foundation under grant number DMR-96-23181.

References

[1] Fischer K H and Hertz J A 1991 *Spin Glasses* (Cambridge: Cambridge University Press)
[2] Sachdev S 1994 *Phys. World* **7** (10) 25
[3] Finkelstein A M 1983 *Sov. Phys.–JETP* **57** 97; 1984 *Z. Phys.* B **56** 189
Altshuler B L and Aronov A G 1983 *Solid State Commun.* **46** 429
Castellani C and DiCastro C 1985 *Localization and the Metal–Insulator Transition* ed H Fritzsche and D Adler (New York: Plenum)
[4] Quirt J D and Marko J R 1971 *Phys. Rev. Lett.* **26** 318
Ue S and Maekawa S 1971 *Phys. Rev.* B **3** 4232
Alloul H and Dellouve P 1987 *Phys. Rev. Lett.* **59** 578
Sachdev S 1989 *Phys. Rev.* B **39** 5297
Milovanovic M, Sachdev S and Bhatt R N 1989 *Phys. Rev. Lett.* **63** 82
Bhatt R N and Fisher D S 1992 *Phys. Rev. Lett.* **68** 3072
Dasgupta C and Halley J W 1993 *Phys. Rev.* B **47** 1126
Dobrosavljevic V and Kotliar G 1993 *Phys. Rev. Lett.* **71** 3218
Lakner M, von Lohneysen H, Langenfeld A and Wolfle P 1994 *Phys. Rev.* B **50** 17 064
[5] Ma S-k, Dasgupta C and Hu C-k 1979 *Phys. Rev. Lett.* **43** 1434
Dasgupta C and Ma S-k 1980 *Phys. Rev.* B **22** 1305
Hirsch J E 1980 *Phys. Rev.* B **22** 5355
Bhatt R N and Lee P A 1982 **48** 344
[6] Lamelas F J, Werner S A, Shapiro S M and Mydosh J A 1995 *Phys. Rev.* B **51** 621
[7] Hertz J A 1979 *Phys. Rev.* B **19** 4796
[8] Oppermann R and Binderberger M 1994 *Ann. Phys., Lpz.* **3** 494
[9] Sachdev S, Read N and Oppermann R 1995 *Phys. Rev.* B **52** 10 286
[10] Sengupta A and Georges A 1995 *Phys. Rev.* B **52** 10 295
[11] Read N, Sachdev S and Ye J 1995 *Phys. Rev.* B **52** 384
[12] Sachdev S and Ye J 1992 *Phys. Rev. Lett.* **69** 2411
[13] Sachdev S and Ye J 1993 *Phys. Rev. Lett.* **70** 3339
[14] Georges A, Kotliar G, Krauth W and Rozenberg M J 1996 *Rev. Mod. Phys.* **68** 13
[15] Huse D A and Miller J 1993 *Phys. Rev. Lett.* **70** 3147
[16] Ye J, Sachdev S and Read N 1993 *Phys. Rev. Lett.* **70** 4011
[17] Binder K and Young A P 1986 *Rev. Mod. Phys.* **58** 801
[18] Bray A J and Moore M A 1980 *J. Phys. C: Solid State Phys.* **13** L655
[19] Fisher M E 1978 *Phys. Rev. Lett.* **40** 1610
[20] Harris A B 1974 *J. Phys. C: Solid State Phys.* **7** 1671
Chayes J T, Chayes L, Fisher D S and Spencer T 1986 *Phys. Rev. Lett.* **57** 2999
[21] Sachdev S 1996 *Preprint*
[22] Sachdev S 1995 *Proc. 19th IUPAP Int. Conf. on Statistical Physics (Xiamen)* (Singapore: World Scientific)
[23] Senthil T and Majumdar S N 1996 *Phys. Rev. Lett.* **76** 3001